Ninth International Conference on CFD in the Minerals and Process Industries
CSIRO, Melbourne, Australia
10-12 December 2012

POPULATION BALANCE MODEL FOR THE CFD SIMULATION OF ADIABATIC AND DIABATIC TWO PHASE GAS LIQUID FLOWS

Eckhard KREPPER and Dirk Lucas

Helmholtz-Zentrum Dresden-Rossendorf, 01314 Dresden, POB 510119, GERMANY
Corresponding author, E-mail address: E. Krepper@hzdr.de

ABSTRACT

A generalized inhomogeneous Multiple Size Group (MUSIG) model based on the Eulerian modeling framework was developed in close cooperation of ANSYS-CFX and Helmholtz-Zentrum Dresden-Rossendorf (HZDR) and implemented into CFX. By simulating a poly-dispersed gas-liquid two-phase flow, the mass exchanged between bubble size classes by bubble coalescence and bubble fragmentation as well as the momentum exchange due to bubble size dependent bubble forces have to be considered. In a vertical pipe flow particularly the radial separation phenomenon of small and large bubbles, which was proven to be a key phenomenon for the establishment of the corresponding flow regime, is well described by this approach. Recently the approach was extended by including bubble shrinking or growing by condensation or evaporation. Size dependent bubble forces can at least be represented roughly by assigning the size groups to few different dispersed gaseous phases having different velocity fields.

The derived model has been validated against experimental data from the TOPFLOW test facility at the HZDR. Numerous tests investigating air-water flow at 0.25 MPa and steam-water flow at steam pressures between 1-6.5 MPa and sub-cooling temperatures from 2 to 17 K in vertical pipes having a length up to 8 m and a diameter up to 200 mm were performed. The wire-mesh technology measuring local gas volume fractions, bubble size distributions and velocities of gas and liquid phases at different distances from the gas injection was applied.

For air/water flow the shift of the gas volume fraction profile from a wall peak to core peak could be reproduced. For steam water flow by varying the gas nozzle diameter the initial bubble size was influenced and the effect of the bubble size on the condensation rate could be shown. Due to the drop of hydrostatic pressure along the pipe, the saturation temperature falls towards the upper pipe end and for some tests in the upper part re-evaporation was reproduced.

Weaknesses in this approach can be attributed to the characterization of bubble coalescence and bubble fragmentation, which must be further investigated. A further topic is bubble induced turbulence.

NOMENCLATURE

a_i specific interfacial area [m^{-1}]
C_L lift force coefficient [-]
d bubble diameter [m]
Eo Eötvös number [-]
$F_{B/C}$ Break-up, coalescence coefficients [-]
F_L lift force [kg m s^{-2}]
h heat transfer coefficient [J m^{-2} s^{-1}]
H evaporation heat [J K^{-1}]
J superficial velocity [m s^{-1}]
N number of velocity groups [-]
M number of sub-size groups [-]
Nu Nusselt number [-]
Re Reynolds number [-]
T Temperature [K]
T_{sat} Saturation temperature [K]
V velocity [m s^{-1}]
w bubble velocity [m s^{-1}]
z axial coordinate [m]

_B bubble
_l liquid
_g gas

α volumetric fraction [-]
σ Surface tension [N m^{-1}]
ρ density [kg m^{-3}]
$\mathbf{u}$ velocity [m s^{-1}]

INTRODUCTION

Many flow regimes in industrial processes are characterized by multiphase flows, with one phase being a continuous liquid and the other phase consisting of gas or vapour of the liquid phase. The flow regimes found in vertical pipes vary from bubbly flows at low fractions to higher void fraction regimes of slug flow, churn turbulent flow, annular flow and finally to droplet flow. In the regime of bubbly and slug flow the multiphase flow shows a spectrum of different bubble sizes. While disperse bubbly flows with low gas volume fraction are mostly mono-disperse, an increase of the gas volume fraction leads to a broader bubble size distribution due to breakup and coalescence of bubbles. Bubbles of different sizes are subject to lateral migration due to forces acting in lateral direction, which is different from the main drag force direction. Further the bubble lift force was found to change the sign as the bubble size varies. Consequently this lateral migration leads to a radial de-mixing of small and large bubbles and to further coalescence of large bubbles migrating towards the pipe center into even larger Taylor bubbles or slugs.

An adequate modeling approach has to consider all these phenomena. The paper presents a generalized inhomogeneous Multiple Size Group (MUSIG) Model based on the Eulerian modeling framework. Within this

model the dispersed gaseous phase is divided into N inhomogeneous velocity groups (phases) and each of these groups is subdivided into Mj bubble size classes. Bubble breakup and coalescence processes between all bubble size classes Mj are taken into account by appropriate models.

THE INFLUENCE OF THE LATERAL LIFT FORCE ON THE FLOW REGIME

In simulating a two-phase flow by applying the Euler/Euler approach, the momentum exchange between the phases must be considered. Apart from the drag acting in flow direction, the so-called non-drag forces acting mostly perpendicular to the flow direction must also be considered. Namely the lift force, the turbulent dispersion force and the wall force play an important role. The turbulent dispersion force considers the turbulent mixing of the bubbles and consequently acts to smooth the spatial gas fraction distribution. The wall force reflects the need for a repelling effect of the wall on bubbles. A more detailed discussion on these forces and their validity for vertical pipe flow can be found in Lucas et al. (2007).

Lift force inversion in a poly-disperse bubbly flow

The lift force considers the interaction of the bubble with the shear field of the liquid per unit volume and can be calculated as:

$$\vec{F}_L = -C_L \rho_l \alpha (\vec{u}_g - \vec{u}_l) \times rot(\vec{u}_l) \qquad (1)$$

The classical lift force formulation for two-phase flows, which has a positive coefficient C_L, acts in the direction of decreasing liquid velocity. In the case of co-current upward pipe flow, this is the direction towards the pipe wall. Numerical (Ervin and Tryggvason, 1997, Bothe et al., 2006) and experimental (Tomiyama et al., 1995) investigations have shown that the direction of the lift force changes its sign for gas-liquid flows if a substantial deformation of the bubbles occurs. Tomiyama (1998) investigated single bubble motion and derived the following correlation for the coefficient of the lift force from these experiments:

$$C_L = \begin{cases} \min[0.288\tanh(0.121\,\mathrm{Re}),\, f(Eo_d)] & Eo_d < 4 \\ f(Eo_d) & \text{for} \quad 4 < Eo_d < 10 \\ -0.27 & Eo_d > 10 \end{cases} \qquad (2)$$

$$\text{with} \quad f(Eo_d) = 0.00105 Eo_d^3 - 0.0159 Eo_d^2 - 0.0204 Eo_d + 0.474$$

This coefficient depends on the modified Eötvös number given by:

$$Eo_d = \frac{g(\rho_l - \rho_g) d_h^2}{\sigma} \qquad (3)$$

Here d_h is the maximum horizontal dimension of the bubble. It is calculated using an empirical correlation for the aspect ratio by Wellek et al. (1966):

$$d_h = d_B \sqrt[3]{1 + 0.163 Eo^{0.757}} \qquad (4)$$

Figure 1 represents the dependency of C_L on the bubble size for an air-water system under ambient conditions as calculated by in eq. (2). For this case C_L changes its sign at a bubble diameter of d_b = 5.8 mm.

The MTLoop and the TOPFLOW experiments performed at HZDR (Prasser et al. 2007, Lucas et al. 2007) have shown that the lift force reverses in an evolving poly-disperse bubbly flow in an upward vertical pipe as well. Radial void fraction distributions decomposed according to the bubble size show a wall peak for bubbles below the critical diameter, while bubbles with a larger diameter form a central void fraction peak. This is independent of the general type of profile of the total void fraction, i.e. a wall-peak for the fraction of small bubbles is also found with a pronounced central peaked total void fraction profile.

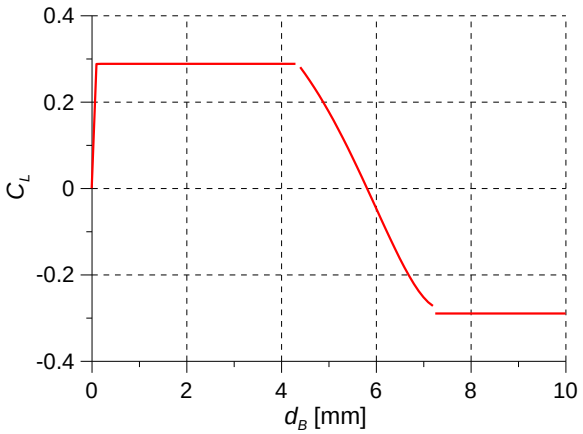

Figure 1: Lift coefficient for air-water bubbly flow according to eq. (2)

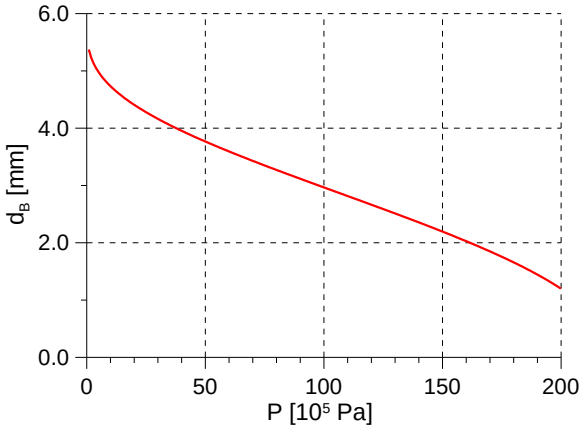

Figure 2: Decrease of the critical equivalent bubble diameter of the lift force sign change for steam-water bubbly flow vs. increasing saturation pressure

Keeping in mind that the surface tension decreases with growing saturation temperature, the critical bubble diameter is expected to be lower for the steam-water tests. The dependency is given in Fig. 2. This was confirmed by the measurements.

Development of the flow along a vertical pipe – radial separation of large and small bubbles

The evolution of the flow along the pipe is determined by a complex interaction between the bubble forces, which has the effect of a lateral bubble migration and the bubble coalescence and breakup. Furthermore, the transition from bubbly to slug flow is influenced by this interaction. As mentioned above the lift force causes, that small bubbles (diameter < ca. 5.8 mm in case of air-water flow) can be found preferably in the wall region, while larger bubbles

are accumulated in the core region. This separation of small and large bubbles clearly influences the development of the flow, since bubble coalescence and breakup depends on the local bubble number densities of the bubbles (see Prince and Blanch 1990, Luo and Svendsen 1996). On the other hand, the dissipation rate of turbulent energy is clearly larger in the near wall region than in the core flow.

The consequences for the transition to slug flow can be explained by the help of Fig. 3. where an upward air-water flow is considered. In both of the cases considered, small bubbles (diameter < 5.8 mm) are injected. On the left side of the figure, a low superficial gas velocity was assumed. The small bubbles tend to move towards the wall. The local gas fraction in the wall region is larger than the averaged gas fraction, but it is still low. In this case bubble coalescence and breakup are in equilibrium and a stable bubbly flow is established.

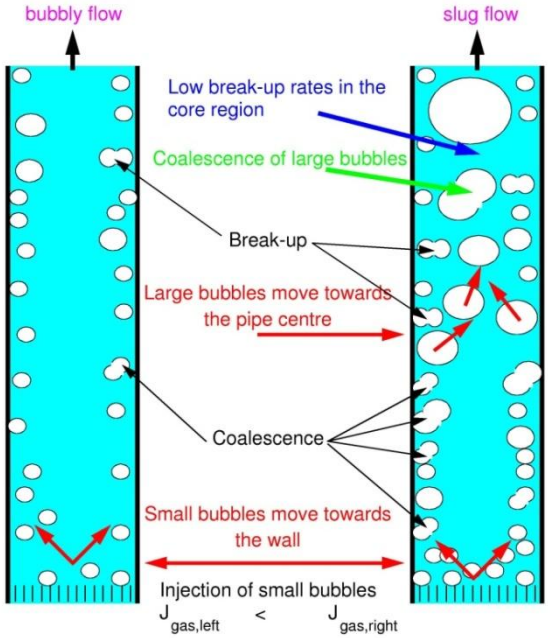

Figure 3: Stable bubbly flow (left) and transition to slug flow (right) (from Lucas et al., 2003)

If the gas superficial velocity is increased (Fig. 3, right side), the equilibrium between bubble coalescence and breakup is shifted towards a larger bubble diameter, because the coalescence rate increases as the square of the bubble number density, while the breakup rate is only proportional to the bubble density. However, the bubble breakup rate strongly increases with the bubble diameter.

By a further increase of the gas superficial velocity, more and more large bubbles (diameter > 5.8 mm) are generated. They start to migrate towards the pipe centre. If enough large bubbles are generated by coalescence in the wall region, some of them can reach the core region without further breakup. Due to the lower dissipation rate of turbulent energy, the bubbles can then grow in size owing to further coalescence events with corresponding lower breakup rates, which is typical of the low shear flow in the pipe centre.

This is the key mechanism for the transition from bubble to slug flow. That means, that for an appropriate model describing this regime transition, a number of bubble size classes as well as radial gas fraction profiles for each bubble size class and the lateral migration of differently sized bubbles must be considered.

MULTIPLE SIZE GROUP APPROACH

For larger gas volume fractions, several bubble size classes have to be considered and the exchange of mass between them caused by bubble coalescence and breakup phenomena has to be taken into account. In principle, the Eulerian two-fluid approach as described above can be extended to simulate a continuous liquid phase and several gaseous dispersed phases by solving the complete set of balance equations for each phase. The investigations however showed that for an adequate description of bubble fragmentation and bubble coalescence a population balance model based on decades of bubble size classes would be necessary. In a CFD code, such a procedure is limited by the increased computational effort to obtain converged flow solutions.

A combination of the consideration of different dispersed phases and the algebraic multiple size group model was proposed to combine both the adequate number of bubble size classes for the simulation of coalescence and breakup and a limited number of dispersed gaseous phases to limit the computational effort (Krepper et al. 2005). The inhomogeneous MUSIG model was developed in cooperation with ANSYS CFX, implemented in CFX (Shi et al. 2004, Frank et al. 2005) and validated (Frank et al. 2008, Krepper et al. 2008).

In the inhomogeneous MUSIG model the gaseous disperse phase is divided into a number N of so-called velocity groups (or phases), where each of the velocity groups is characterized by its own velocity field. Furthermore, the overall bubble size distribution is represented by dividing the bubble diameter range within each of the velocity groups j into a number of sub-size fractions M_j $j=1..N$. The population balance model considering bubble coalescence or bubble breakup is applied to the sub-size groups (see Fig. 4).

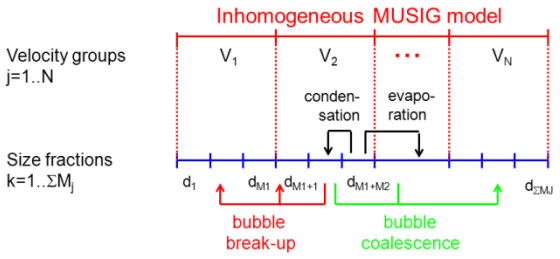

Figure 4: Schematic of the inhomogeneous MUSIG approach: The size fractions M_j are assigned to the velocity field V_i

The subdivision should be based on the physics of bubble motion for bubbles of different size, e.g. different behavior of differently sized bubbles with respect to bubble forces. The strongest influence of the bubble size on any bubble force was found on the lift force. Dependent on the flow situation in most cases N=2 for bubbles smaller respective larger the critical diameter for which the lift force coefficient changes the sign are sufficient in order to capture the main phenomena.

Coalescence and breakup

The net mass source for size group i due to bubble coalescence and breakup can be expressed as the sum of bubble birth rates due to the breakup of larger bubbles

from groups $j > i$ to group i and coalescence of smaller bubbles from size groups $j < i$, to group i as well as bubble death rates due to breakup of bubbles from size group i to smaller bubbles in groups $j < i$ and the coalescence of bubbles from size group i with bubbles from any other group to even larger ones which belong to groups $j > i$. The birth and death rates in turn are commonly expressed in terms of the coalescence and breakup kernels. For the breakup and coalescence kernel functions the commonly used breakup models according to Luo and Svendsen (1996) and the coalescence models of Prince and Blanch (1990) are applied in the present work, but were adjusted by factors to match the measured bubble sizes. In this way only the applicability of the general framework is demonstrated but of course further developments will be necessary to improve the physical models and overcome such tuning procedures.

Condensation and evaporation

When condensation or evaporation occur, the volume fraction in size group i changes for two reasons: (a) mass is transferred directly between the bubbles and the liquid and (b) since due to this direct mass transfer the bubbles are shrinking or growing they may subsequently belong to a different size group.
Written as a source term for size group i the direct mass transfer to the liquid is given by

$$\tilde{\Gamma}_i = -\frac{A_{I,i}}{H_{LG}} h_{L,i}(T_L - T_{sat}) \tag{5}$$

where the assumption has been made that the gas is at saturation temperature. The total source terms for size class i including also the ensuing change of bubble size, i.e. $\tilde{\Gamma}_i^{phase}$ in Eq. (5), has been derived recently by Lucas et al (2011)

$$\Gamma_i^{phase} = \frac{m_i}{m_i - m_{i-1}} \tilde{\Gamma}_i - \frac{m_i}{m_{i+1} - m_i} \tilde{\Gamma}_{i+1}$$

for $\tilde{\Gamma}_i < 0$, i.e. condensation respective (6)

$$\Gamma_i^{phase} = \frac{m_i}{m_i - m_{i-1}} \tilde{\Gamma}_{i-1} - \frac{m_i}{m_{i+1} - m_i} \tilde{\Gamma}_i$$

for $\tilde{\Gamma}_i > 0$, i.e. evaporation.

where $m_i = \rho \pi d_B^{\,3} / 6$ is the mass of each bubble in size group i. Basing the calculation on bubble mass rather than size for compressible flows has the advantage that since mass is conserved no extra terms arise in the equations. Conversion to the corresponding bubble size which depends on the local density can be done straight forwardly as needed. For incompressible flows, no differences between mass- and size-based groups arise.

EXPERIMENTS AT THE TOPFLOW FACILITY

Gas-liquid flow in vertical pipes is a very good subject for studying the phenomena of gas-liquid two-phase flows. In case of bubbly flows the bubbles move under well determined boundary conditions, resulting in a shear field of constant and well-known structure where the bubbles rise for a comparatively long time. This allows studying the lateral motion of the bubbles in a shear flow by comparing gas distributions measured at different heights.
Experiments are done using the TOPFLOW facility of the HZDR. The facility allows producing up to 1.4 kg/s saturated steam at the maximum operational pressure of 7 MPa by a 4 MW electrical steam generator (Prasser et al. 2006). Several test rigs are operated at the facility. For investigations of two-phase flow characteristics in vertical pipes wire-mesh sensors are used. This technology is intrusive, i.e. it influences the two-phase flow. For this reason it is not possible to place several sensors behind each other to investigate the evolution of the flow along the pipe. Instead in the experiments to investigate the evolution of the flow the measuring plane is always at the upper end of the pipe. Performing different tests at the same boundary conditions but injecting gas at different distances from this measuring plane through orifices in the pipe wall, the evolution can be investigated.

SETUP OF THE CFD SIMULATIONS

For the simulation the CFD code CFX in the version 12.1 applying the standard framework of Euler/Eulerian two phase flow was adopted.
The drag force according to Grace (Clift et al. 1978) was used. The turbulent dispersion force according to Burns (2004) and the wall force model of Antal (1991) were applied. For the lift force the correlation of Tomiyama (1998) with its bubble size dependent lift force coefficient was used. Whereas for air/water a sign change of the lift coefficient at $d_B \approx 6$ mm could be observed, this critical diameter for vapour/water is shifted towards smaller values. For 2 MPa a critical diameter of $d_B \approx 4.5$ mm was found.
A 2D cylinder symmetric geometry was used to reduce the computational effort. The experimental results at level A (0.221 m distance from steam injection) were used as inlet condition of the simulation. These concerns the cross sectional averaged bubble size distribution, the radial vapour volume fraction profile and the radial vapour velocity profile. For the level A a constant velocity difference between water and vapour was adjusted so that the specified superficial velocities are met. Inlet conditions for the radial profiles of turbulent kinetic energy and turbulent dissipations were set. These profiles were determined performing a previous single phase calculation. At the outlet a pressure boundary condition was set so that the absolute pressure corresponds to the experimental specifications. The simulations were run with a steady state assumption.

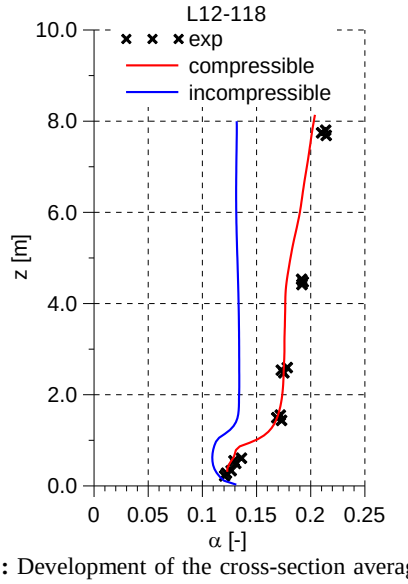

Figure 5: Development of the cross-section averaged gas volume fraction with height z

SIMULATING TWO PHASE FLOW IN VERTICAL PIPES

Air Water Flow

For the TOPFLOW test, the gas was considered as compressible, which results in a hydrostatic pressure caused increase of the void fraction with the height (see Fig. 5).

Bubbles were injected from the side walls through 4 mm nozzles into a tube of diameter 195.3 mm. The bubble size distribution near the inlet shows large fractions of large bubbles (Fig. 6, size distribution at level A). During the upward flow through the tube the size distribution is shifted towards lower values. Thus in this example the development of the bubble size distribution is mainly determined by fragmentation processes. Bubble coalescence plays only a minor role at the flow conditions of the experimental test. Fig. 6 shows the bubble size distribution and radial gas profiles for the test case TOPFLOW 118 for a quite low distance from the gas injection of 0.221 m (level A) and at a distance of 7.802 m (level R). Note that only two dispersed phases were defined for the numerical model. 20 sub-size groups were then specified, where the first 2 sub-size groups are assigned to the first dispersed phase and the other 18 are assigned to the second dispersed phase. The bubble size diameter was defined up to 60 mm, the size step between the sub-size groups is equal to 3 mm. Test calculations have shown, that setting the breakup coefficient to F_B=0.25 and the coalescence coefficient to F_C=0.05 yields the best agreement for this flow regime of air-water flow in vertical pipes. Both the shift of the bubble size distribution (Fig. 6 left side) and the core peak gas volume fraction profile are well reproduced by the calculations.

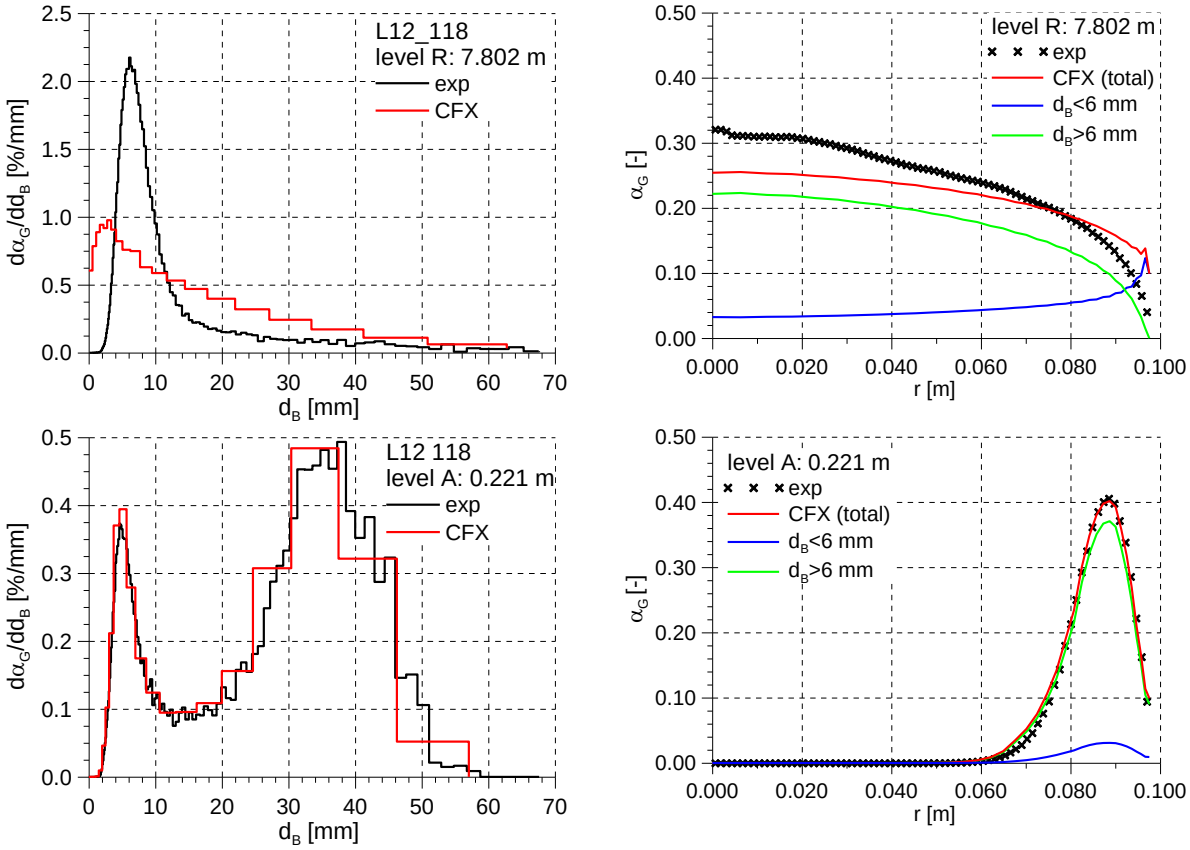

Figure 6: Development of the bubble size distribution (left) and the radial gas fraction profiles (right) for the simulation of the test case TOPFLOW L12-118, (J_L=1.017 m/s; J_G=0.2194 m/s) 2 dispersed phases, 21 MUSIG Groups (F_B=0.25, F_C=0.05)

Steam-water flow

Earlier investigations of steam/water tests at saturation conditions had shown, that applying the same models for bubble fragmentation like for air/water the calculated bubble fragmentation rate exceeds the measured values. Therefore as a first step during these calculations bubble fragmentation and coalescence were neglected. Only the change of gas fraction and bubble size distribution by mass transfer (condensation respective evaporation) was considered.

The bubble-liquid heat transfer coefficient

During the simulations the vapour was assumed to be at saturation conditions, whereas for the liquid phase the energy equation was solved. In general correlations for the heat transfer model between vapour bubbles and liquid have the following form:

$$Nu = 2 + c \cdot \mathrm{Re}^{\alpha}\ \mathrm{Pr}^{0.3} \qquad (7)$$

Three different correlations have been used here: a) Ranz-Marshall (1952) correlation (c=0.6, α=0.2) is only recommended for small Reynolds number (Re<780). b)

Hughmark (1967) suggests for larger Reynolds number c=0.27 and α=0.62, whereas c) Tomiyama (2009) proposes c=0.15 and α=0.8 for all Re.
In Fig. 7 the cross sectional averaged vapour void fractions as a function of the tube height z are shown. The graphs of the measured as well as the simulated values for this condensation dominated test case are approximately straight lines in the semi logarithmic plot. This means that the steam void fraction decreases approximately exponentially with the height.
Fig. 7a shows the sensitivity of the calculated vapour volume fraction to the choice of the heat transfer model. . A slight overestimation of the vapour void fraction for the Ranz Marshall correlation and a strong underestimation for the Tomiyama correlation was calculated for test case 118_dt6_1. The best agreement was found for the correlation according to Hughmark. In the following simulations this correlation was used.

Influence of increasing the initial bubble size distribution

For the tests 118_dt6_1 and 118_dt6_4 almost all vapour in the experiments is condensed after half of the height. Therefore for this test only half of the tube length was simulated. Figures 8 and 9 show the cross sectional averaged bubble size distribution and the radial vapour profiles. The vapour is injected from the side (at R=D/2=0.098 m). In both tests the vapour is remaining near the wall (see Figs 8b and 9b). Caused by the higher interfacial area for smaller bubble sizes the condensation rate for the 1 mm nozzle size test is higher than for the 4 mm tests. Consequently the steam void fraction is lower (see Fig. 9b for the cross sectional averaged values). Whereas the bubble size distribution in the test 118_dt6_1 is calculated with reasonable agreement to measurements, the size distribution for the 4 mm case is overestimated with respect to bubble sizes and vapour void fraction (see Fig. 9, level H). Consequently for this test the cross sectional averaged vapour fraction is calculated too large. For this test bubble fragmentation might play a role. For both tests the small size bubble velocity class plays only a limited role. In principle these tests could also calculated applying a homogeneous MUSIG approach.

Simulation of a test with evaporation

During some tests an increasing vapour volume fraction by re-evaporation with increasing height was observed (see Fig. 10a). This was the case when the inlet temperature was very close to the saturation temperature. With increasing height the hydrostatic pressure decreases and the saturation temperature falls below the liquid temperature (see Fig. 10b). In these cases the exact values of the inlet temperature have a very sensitive influence on the further development of the flow. Furthermore the errors of the temperature measurements are in the order of magnitude of the subcooling temperature. The test specification for subcooling was related to z=0, whereas in the simulation the inlet condition at level A has to be set. The sensitive influence of the inlet subcooling temperature set at level A was investigated (see Fig. 10a for the cross sectional averaged vapour void fraction and Fig. 10b for the cross sectional averaged liquid temperature). Depending on the inlet temperature also in the calculations re-evaporation could be observed.

CONCLUSIONS

The application of the inhomogeneous MUSIG approach enables the rough consideration of a dependency of the bubble size on the momentum exchange between gas and liquid. In a vertical gas liquid pipe flow the radial separation of small and large bubbles can be described, which is a key phenomenon for the establishment of a certain flow regime.

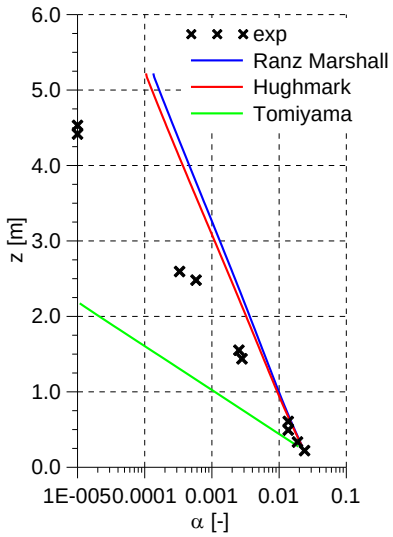

a) Influence of the heat transfer model, (Nozzle diameter: D_{Nozzle}=1mm)

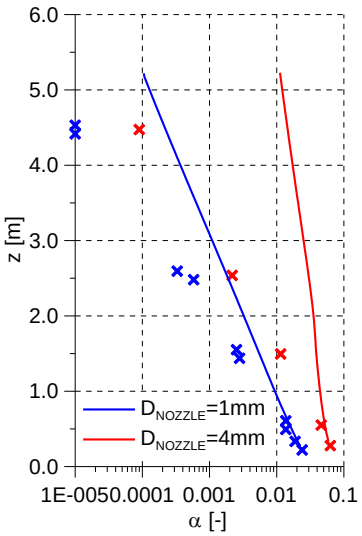

b) Influence of the initial bubble size distribution. (D_{Nozzle}=1 versus 4mm)

Figure 7: Cross sectional averaged vapour void fractions for tests 118_dt6 (T_{SUB}=6K)

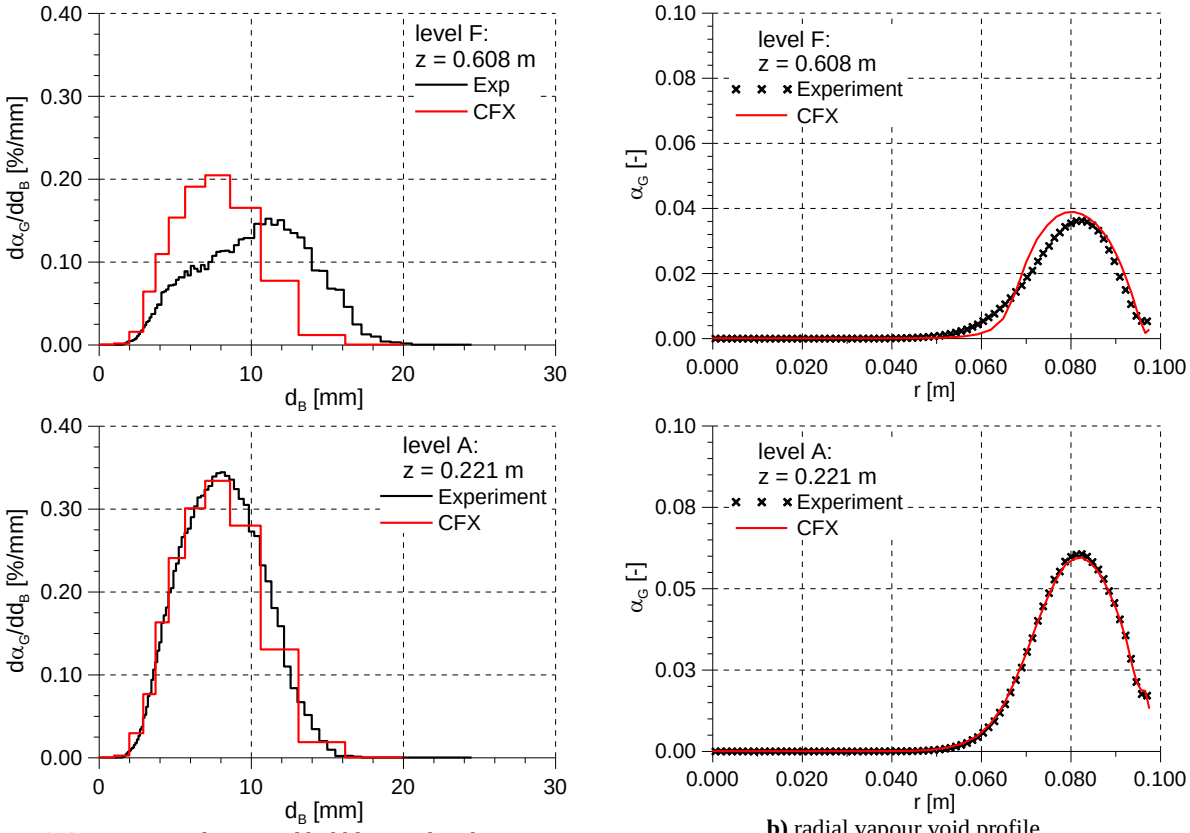

a) Cross sectional averaged bubble size distribution

b) radial vapour void profile

Figure 8: Development of the vapour void at different distances z from the steam injection. Test 118_dt6_1 (T_{SUB} = 6K, D_{Nozzle} = 1mm)

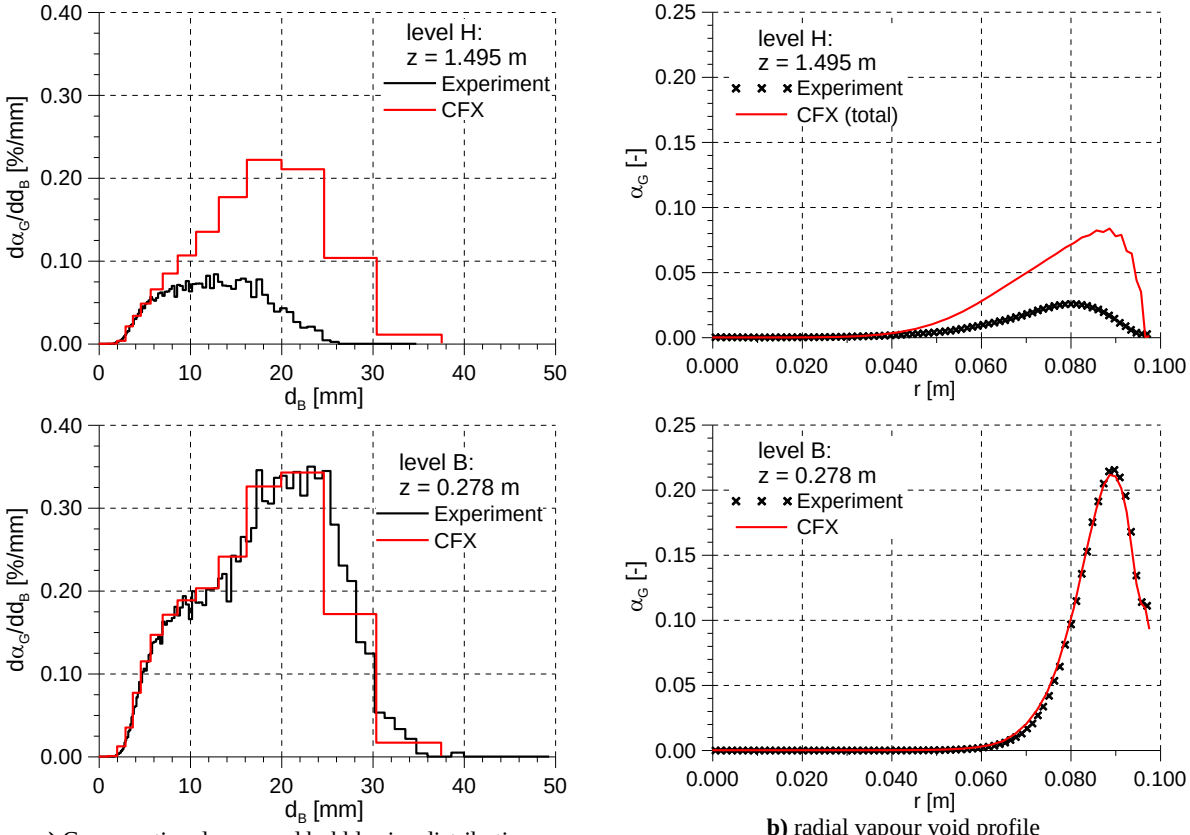

a) Cross sectional averaged bubble size distribution

b) radial vapour void profile

Figure 9: Development of the vapour void at different distances z from the steam injection. Test 118_dt6_4 (Tsub = 6K, DNozzle = 4mm)

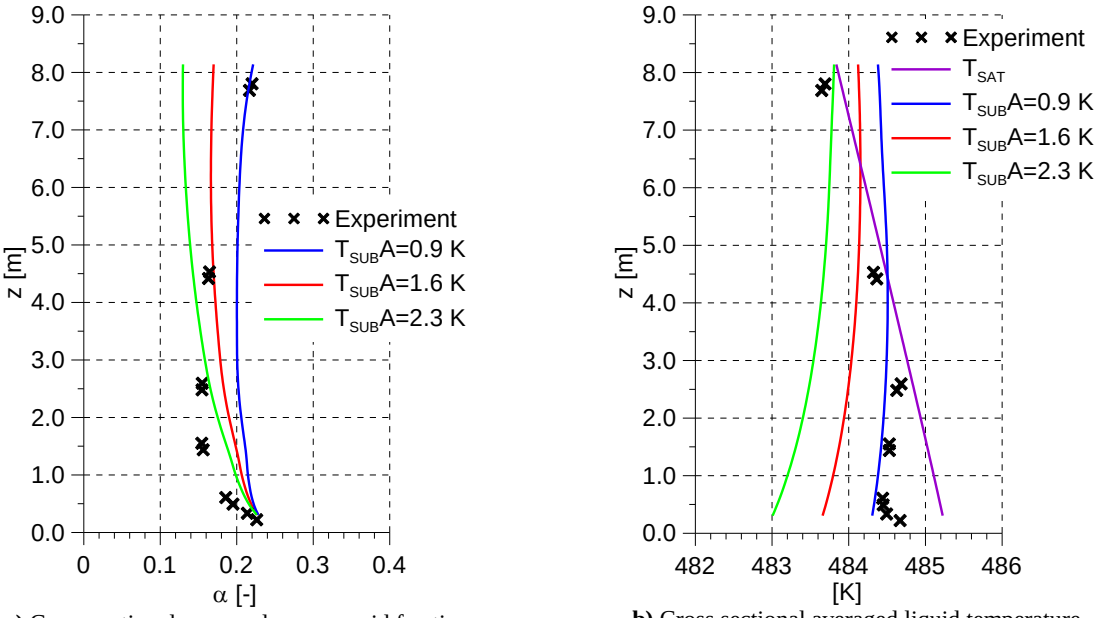

a) Cross sectional averaged vapour void fraction

b) Cross sectional averaged liquid temperature

Figure 10: Symbols: Experiment: Test 140_dt3.2_1. Lines: Calculations for various T_{SUB}

The CFD simulation of the condensation of steam bubbles in water can be improved considering the bubble size distribution. The extension of the multiple bubble size group approach (MUSIG) by mass transfer is described. Experiments performed at TOPFLOW are described which are capable to validate the implemented models.

The simulation of some selected tests and comparison to measurements is described. The correct operation of the model could be shown. Earlier and also the actual investigations show for vapour/water flow an overestimation of bubble fragmentation applying the same models like for air/water flow. To limit the influences in the presented simulation, as a first step, vapour bubble fragmentation and coalescence were neglected. The influence of the heat transfer model between bubbles and liquid was investigated. The best agreement for the cross sectional averaged vapour void fraction compared to the measurements was found applying the heat transfer correlation proposed by Hughmark. The commonly correlation Ranz and Marshall predicts a slightly lower heat condensation whereas the correlation by Tomiyama calculates significantly higher condensation then experimentally observed. The simulations were extended to tests with larger initial bubble sizes produced with larger injection nozzles. Here the Hughmark model underestimates the condensation and the bubble shrinking. In this case bubble fragmentation may play a role, because it increases the interfacial area and thereby the condensation. Bubble fragmentation and coalescence will be considered in the future work. In some tests cases with inlet liquid temperatures close to saturation, after some condensation close to the inlet, further downstream a re-evaporation can be observed. This phenomenon is caused by the drop of saturation temperature due to the decreasing hydrostatic pressure along the pipe height. The simulation of these processes depends on the setting of the inlet temperature very sensitively. Further investigations are necessary.

ACKNOWLEDGMENTS

This work was funded by the German Federal Ministry of Economics and Labour, project numbers 150 1329 and 150 1411. The authors like to thank all members of the TOPFLOW team who contributed to the successful performance of these experiments.

REFERENCES

ANTAL, S.; LAHEY, R. & FLAHERTY, J., 1991. Analysis of phase distribution in fully developed laminar bubbly two-phase flow, International Journal of Multiphase Flow, 17, 635

BOTHE, D., M. SCHMIDTKE, H.-J. WARNECKE (2006) VOF-Simulation of the Lift Force for Single Bubbles in a Simple Shear Flow, Chem. Eng. Technol. 29, No. 9, 1048–1053

BURNS, A. D., FRANK, T., HAMILL, I., SHI, J.-M., 2004. The Favre Averaged Drag Model for Turbulent Dispersion in Eulerian Multi-Phase Flows, 5th International Conference on Multiphase Flow, ICMF'04, Yokohama, Japan, May 30–June 4, 2004, Paper No. 392.

CLIFT, R., GRACE, J.R., WEBER, M.E., 1978. Bubble Drops and Particles, Academic Press New York

ERVIN, E.A., TRYGGVASON, G. (1997). The rise of bubbles in a vertical shear flow, J.l of Fluids Engineering, vol. 119, pp. 443-449.

FRANK, T., ZWART, P.J., SHI, J.-M., KREPPER, E., ROHDE, U. 2005. Inhomogeneous MUSIG Model – a Population Balance Approach for Polydispersed Bubbly Flows, International Conference "Nuclear Energy for New Europe 2005", Bled, Slovenia, September 5-8, 2005.

FRANK, T., ZWART, P., KREPPER, E., PRASSER, H.-M. & LUCAS, D., 2008. Validation of CFD models for

mono- and polydisperse air–water two-phase flows in pipes, Nuclear Engineering and Design, 238, 647-659

HUGHMARK, G. A., 1967. Mass and Heat Transfer from Rigid Spheres, AlChE Journal, 13, 1219

KREPPER, E., LUCAS, D., PRASSER, H.-M., 2005. On the modelling of bubbly flow in vertical pipes, Nuclear Engineering and Design, 235, 597-611

KREPPER, E., LUCAS, D., FRANK, T., PRASSER, H.-M., ZWART, P., 2008. The inhomogeneous MUSIG model for the simulation of polydispersed flows, Nuclear Engineering and Design, 238, 1690-1702

LUCAS, D., KREPPER, E., PRASSER, H.-M., 2003. Evolution of flow patterns, gas fraction profiles and bubble size distributions in gas–liquid flows in vertical tubes. Trans. Inst. Fluid-Flow Machinery 112, 37–46.

LUCAS, D., KREPPER, E., PRASSER, H.-M., 2007. Use of models for lift, wall and turbulent dispersion forces acting on bubbles for poly-disperse flows, Chemical Science and Engineering, 62, 4146-4157

LUCAS, D., M., FRANK, T., LIFANTE, C, ZWART, P., BURNS, A., 2011. Extension of the inhomogeneous MUSIG model for bubble condensation. Nuclear Engineering and Design 241, 4359–4367

LUO, H. and SVENDSEN, H.F. (1996), Theoretical model for drop and bubble break-up in turbulent flows, AIChEJ, 42, 5, pp. 1225-1233

PRASSER, H.-M.; BÖTTGER, A.; ZSCHAU, J., 1998. A new electrode-mesh tomograph for gas-liquid flows, Flow Measurement and Instrumentation 9, 111-119

PRASSER, H.-M., BEYER, M., CARL, H., MANERA, A., PIETRUSKE, H., SCHÜTZ, P., WEIß, F.-P., 2006. The multipurpose thermal-hydraulic test facility TOPFLOW: an overview on experimental capabilities, instrumentation and results, Kerntechnik, 71, 163-173

PRASSER, H.-M., BEYER, M., CARL, H., GREGOR, S., LUCAS, D., PIETRUSKE, H., SCHÜTZ, P., WEISS, F.-P., 2007. Evolution of the structure of a gas–liquid two-phase flow in a large vertical pipe", Nuclear Engineering and Design, 237, 1848–1861

PRINCE, M.J. AND BLANCH, H.W. (1990), Bubble coalescence and break-up in air-sparged bubble columns, AIChEJ, 36, No 10, pp. 1485-1499

RANZ, W.E., MARSHALL, W.R., 1952. Evaporation from drops, part I, part II, Chemical engineering progress Vol. 48 No. 3, pp. 141

SHI, J.-M., ZWART, P.-J., FRANK, T., ROHDE U. AND PRASSER, H.-M. (2004). Development of a multiple velocity multiple size group model for poly-dispersed multiphase flows. In Annual Report of Institute of Safety Research. Forschungszentrum Rossendorf, Germany, 2004.

TOMIYAMA, A. SOU, I. ZUN, I. KANAMI, N. SAKAGUCHI, T. (1995). Effects of Eötvös number and dimensionless liquid volumetric flux on lateral motion of a bubble in a laminar duct flow, Advances in Multiphase Flow, pp. 3-15.

TOMIYAMA, A., 1998. Struggle with computational bubble dynamics, 3rd Int. Conf. on Multiphase Flow, ICMF'98, Lyon, France

TOMIYAMA, A., 2009. Progress in Computational Bubble Dynamics, 7th Workshop on Multiphase Flow, May 27, Rossendorf

WELLEK, R.M., AGRAWAL, A.K., SKELLAND, A.H.P., (1966). Shapes of liquid drops moving in liquid media, AIChE Journal, vol. 12, pp. 854-860.

